



Numerical Investigation of Thermomechanical Fatigue Behavior in Aero-derivative Gas Turbine Blades

A. M. Orah^{1, 2}; A. Nasir²; A. B. Hassan²; I. Bori²

¹Department of Mechanical Engineering Technology, Federal Polytechnic Kaura Namoda, Zamfara State, Nigeria.

²Department of Mechanical Engineering, Federal University of Technology, Minna, Niger State, Nigeria

Corresponding Author: orahmohammed@yahoo.com; 08028198356

Article Info

Keywords:

Blade, Thermo-Mechanical Fatigue, Heat transfer, Thermal, Stress

Received 01 August 2021

Revised 17 August 2021

Accepted 24 August 2021

Available online 31 August 2021



<https://doi.org/10.37933/nipes/3.3.2021.18>

<https://nipesjournals.org.ng>

© 2021 NIPES Pub. All rights reserved.

Abstract

The hot gas component of the gas turbine engine comprises the burner, the turbine stages, and the exhaust nozzles/ducts. However, the turbine blades experience high thermal and mechanical loading. As a result, they suffer thermo-mechanical fatigue (TMF). The design process usually involves the appropriate selection of the turbine blade materials. Therefore, the need to carry out thermo-mechanical fatigue studies on gas turbine blades to predict blade life. During TMF loading, fatigue, oxidation, and creep damages are induced, and the relative contributions of these damages vary with the different materials and loading conditions. The study employed the finite element method to examine the high temperature and stress effects on the blades during TMF. The blade material considered in this study is a nickel-based super-alloy, Inconel 738 Low Carbon (IN738LC). The finite element method predicted the temperature and stress distributions in the blade, illustrating the blade sections prone to damage during thermomechanical fatigue. The equations from the law of heat conduction of Fourier and the cooling law of Newton predicted the heat transfer process of the interaction between the blade, hot gases, and cooling air. Therefore, the finite element method is suitable for studying the thermomechanical fatigue behavior of turbine blade metals, which is a precursor to blade life predictions.

1. Introduction

Gas turbines employed for producing shaft power are aero-derivative and heavyweight. Aero-derivative gas turbines are direct adaptations of aero engines, with many common parts to produce shaft power. On the other hand, the heavyweight gas turbines are designed with an emphasis on low cost rather than low weight and thus may possess features such as solid rotors and thick casings [1]. The aero-derivative gas turbines adaptation to the electrical generation industry involved removing the bypass fans and installing a power turbine at their exhaust. Their developed power ranges from about 2.5 to 50 MW and could boast of efficiencies up to 45% [2]. Aero-derivative and industrial gas turbines have proven their suitability for heavy-duty, continuous, baseload operation in power generation, pump, and compressor applications [3]. Figure 1 displays the basic principle of operation of a typical gas turbine engine.

The Brayton cycle best describes the gas turbine cycle. Figure 2 illustrates the Temperature-Entropy (TS) diagram of an ideal Brayton cycle. Air is compressed isentropically from point 1 to point 2 and constant pressure heating from point 2 to point 3. Finally, the air expands isentropically from point 3 to point 4 [5].

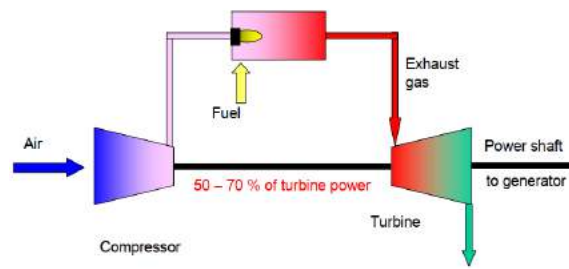


Figure 1: The basic principle of a gas turbine engine. Source: [4]

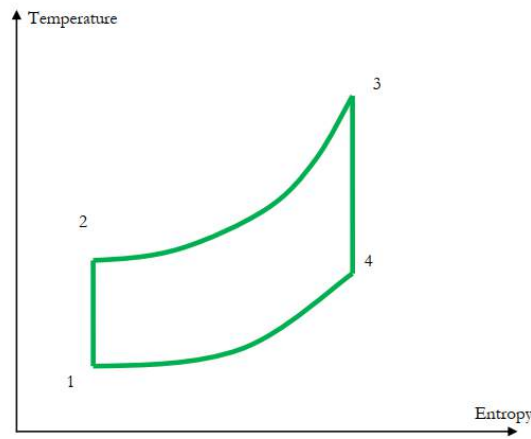


Figure 2: Temperature-entropy (TS) diagram for a closed gas turbine cycle Source:[5]

The Brayton cycle expresses that amplifying the pressure ratio and increasing the turbine's temperature increases the efficiency of the gas turbines. Therefore, the overall efficiency increases by increasing the pressure ratio at a particular temperature [6].

The gas turbine engine is prone to a wide variety of physical problems. These include dirt build-up, fouling, erosion, oxidation, corrosion, foreign object damage, worn bearings, worn seals, excessive blade tip clearances, burned or warped turbine vanes or blades, partially or wholly missing blades or vanes, and a cracked rotor disc or blade [3]. The turbine designer must keep in mind several factors to achieve a high availability and reliability factor. Some of the more critical design considerations are blade and shaft stresses, blade loadings, material integrity, auxiliary systems, and control systems [2]. The operation of a gas turbine engine imposes thermal fatigue loading on the hot section elements leading to subsequent damage to these components, which is one of the main factors governing overhaul intervals. The damage may have a metallurgical or mechanical origin and reduce equipment reliability and availability, increasing the risk of failure [7]. It makes thermo-mechanical fatigue studies essential to predict blade life from the following damage mechanisms: creep, thermal fatigue (low cycle fatigue), thermomechanical fatigue (high cycle fatigue), corrosion, erosion, and oxidation [7]. Thermo-mechanical fatigue (TMF) results by combined thermal and mechanical loading with both the temperatures and stresses varying with time. These types of loadings frequently occur in start-up and shut-down cycles of high-temperature components and equipment [8]. TMF is a form of non-isothermal fatigue in which a material subjects to varied temperatures and independently controlled loading simultaneously. Because the mechanical

properties are temperature dependent, the variation in temperature associated with TMF leads to different damage mechanisms [9]. The thermo-mechanical fatigue test is known to most accurately simulate a gas turbine's substrate [10].

Studies have revealed that the turbine blades and rotor components represent 28 % of the primary causes of gas turbine failures, while 18 % arise from faults in turbine nozzles and stationary parts [11]. Therefore, Nickel-based superalloys find extensive application in the manufacture of hot gas path components in gas turbines used for power generation [12]. The Nickel-based superalloy IN738, developed in 1968, improves gas turbine blades' creep, hot corrosion, and oxidation resistance. Therefore, the performance of thermo-mechanical fatigue tests for IN738LC applied in gas turbine blades for blade life predictions. Several studies on thermo-mechanical fatigue have been done on IN 738LC superalloy. Experimental investigation of the thermo-mechanical fatigue life of uncoated IN738LC nickel-base superalloy performed at a temperature interval of 450-850°C yielded the measurements for stress-strain response and the life cycle of the material. It satisfactorily predicted the thermo-mechanical fatigue lives of the alloy, assuming a plastic strain energy [13]. [14] studied the hysteresis loop of IN738LC using finite element analysis. The results from the hysteresis loop were validated experimentally, and the result was similar to that of the experiment. The hysteresis loop predicted the fatigue life. The predicted fatigue life showed errors of less than 15% [14]. [10] proposed a method for determining the TMF lifetime of IN738LC material using Low Cycle Fatigue (LCF) test results. Then TMF life was estimated using the Ostergren and Zamrik models. Life prediction of IN738LC using the LCF test results from this study was compared with previous lifetime prediction results on the superalloys M963 and GTD-111 to review the cause of the difference in lifetime prediction results. Their results showed that the Ostergren model could predict IP-TMF life with higher accuracy for IN738LC than the Zamrik model. However, the Zamrik model demonstrated higher reliability in predicting life than the Ostergren model [10]

2. Methodology

The study of the thermomechanical fatigue behaviour of the turbine blade material was done in four modules: blade sizing model, thermal model, heat transfer model and stress model. The flow diagram illustrating the TMF process is shown in Figure 3. The finite element method was used to examine the TMF behaviour blade material made of IN738LC. The software employed were the AutoCAD (for CAD modelling), GasTurb (for gas turbine engine performance simulation), and Matlab (for finite element analysis). The composition of Inconel 738LC is shown in Table 1 [15].

Table1: Chemical composition of super-alloy Inconel 738LC (IN738LC)

Element	C	Cr	Mo	Ta	Ti	Al	W	Si	Mn	Nb	Fe	Co	Ni
Weight (%)	0.105	16.00	1.75	1.80	3.40	3.40	2.70	0.09	0.03	0.82	0.30	8.60	Bal

Source: [15]

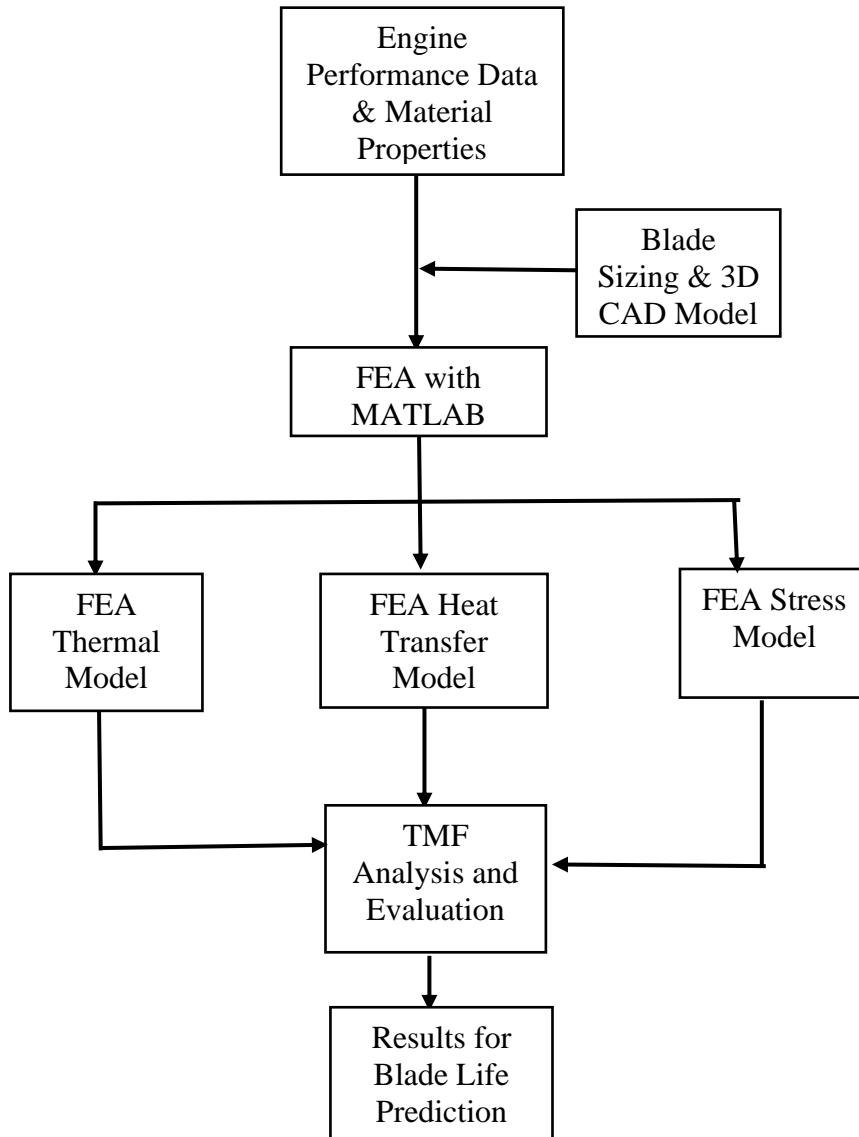


Figure 3: Flow diagram for the TMF Process

The CAD model in Figure 4 describing the blade geometry was produced from the blade dimensions measured from a single spool turboprop aero engine. The dimensions are given in Table 2.

Table 2: Blade Geometry measured from a turboprop aero engine

Dimensions	Value
Height	5.66 cm
Chord	2.54 cm
Thickness	0.15 cm



Figure 4: CAD model of an aero turboprop gas turbine blade

The stereolithographic (STL) model shown in Figure 5 obtained from the CAD model was the basis for the finite element analysis. The STL model displays the face labels and positions, which provides a base for the blade mesh in Figure 6.

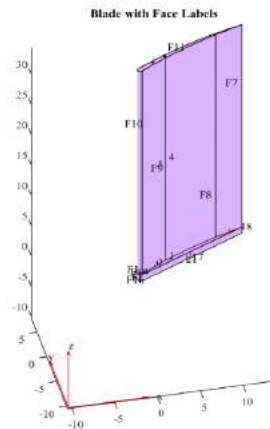


Figure 5: Stereolithographic model of the gas turbine blade showing the face labels

The blade was meshed using finite element (FE) in Matlab with quadratic tetrahedral meshing as shown in Figure 6. The mesh size was 0.50mm and the mesh spacing was 0.005m.

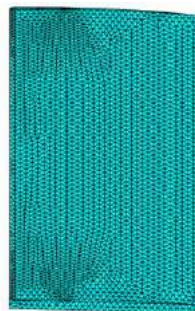


Figure 6: Finite element mesh of the blade model

The parameters considered for the thermal analysis are in Table 3. Some of these parameters were sourced from open literature, while the parameters, specific heat, turbine inlet temperature, turbine exit temperature, pressure ratio, and the heat rate were from the off-design point simulation of a single spool turboshaft engine using GasTurb software.

Table 3: Gas turbine blade parameters for thermal analysis

Parameter	Symbol	Value	Unit
Thermal Conductivity	k	10.1	W/m ² .K
Density of blade material	ρ	7810	kg/m ³
Specific heat capacity	c	455	J/kgK
Turbine inlet temperature	T _g	1073	K
Turbine exit temperature	T _e	549.54	K
Ambient Temperature	T _a	288	K
Coolant temperature	T _c	573	K
Pressure ratio	P	2.15 x 10 ⁶	Pa
Heat rate	Q	13656.1	kJ/kWhr
Cooling hole diameter	D	0.00125	m
Mass flow rate	m	430.65	kg/s
Reynold's number	Re	60000	

Figure 7 shows the Simulink model employed to analyze the blade's thermal loading during the conduction and convective heat transfer process. The heat conduction equation in Equation (1) [16] by Fourier and Newton's law of cooling equation in Equation (2) [17] was necessary for this simulation to examine the heat transfer interaction between the hot gases and the cooling air.

$$q = -k\rho C \left. \frac{dT}{dz} \right|_{z=0} \quad (1)$$

$$q' = Ah_g(T_g - T_w) \quad (2)$$

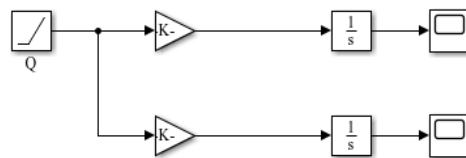


Figure 7: Simulink model for the analysis of conduction and convective heat transfer in the GT blade

The Equations (3) to (5) [18] were used to model the heat transfer on the cold side of the blade using Matlab Simulink.

$$Re_{cs} = \frac{\rho_{cs} \times V_{abscs} \times D_h}{\mu_{cs}} \quad (3)$$

$$Nu_{cs} = 0.15 \times (Re_{cs})^{0.8} \quad (4)$$

$$h_{cs} = Nu_{cs} \left(\frac{k_{cs}}{D_h} \right) \quad (5)$$

Air was assumed as the gas on the cold and hot sides of the blade at temperatures of 573K and 1073k, since the properties are readily available. The Equations (6), (7), (8) and (9) [18] were used to model the heat transfer on the hot side of the blade.

$$Re_g = \frac{\rho_g \times V_{abs} \times C_b}{\mu_g} \text{----- (6)}$$

$$St_g = 0.258 \times (Re_{cs})^{-0.37} \times Pr_g^{-0.667} \text{----- (7)}$$

$$A_g = \pi D_m H C \cos \alpha_2 \text{----- (8)}$$

$$h_g = St_g \times C_{pg} \times \left(\frac{m_g}{A_g} \right) \text{----- (9)}$$

The parameters for the stress analysis on the blade are in Table 4. These parameters were from the simulation results at the off-design point of the turboshaft engine. The stress analysis was done using equation (10). The blade was assumed tapered, and the gas bending stress and centrifugal stress were ignored in this study since they are not very significant [19].

$$(\sigma_{ct})_{max} = \frac{4}{3} \pi N^2 \rho_b A \text{----- (10)}$$

Table 4: Gas turbine blade parameters for stress analysis

Parameter	Symbol	Value	Unit
Speed	N	3610	rpm
Density of blade material	ρ	7810	kg/m ³
Annulus area	A	0.094	m ²
Young's Modulus	E	128.7	GPa
Coefficient of thermal expansion	CTE	0.999	K ⁻¹
Poisson ratio	ν	0.3	
Hot gas pressure	P1	2.24 x 10 ⁶	Pa
Suction side pressure	P2	1.003 x 10 ⁵	Pa

3. Results and Discussion

Continuous heating and cooling cycles cause the blade surface to undergo TMF damage usually caused by internal stresses. The finite element thermal analysis for the heating and cooling cycles at a steady state is in Figure 8. It shows the temperature distribution at each section of the blade span as the cooling air passes through it. It also shows that higher temperatures begin from the mid-span to the top of the blade. The higher temperature region leads to the strain-temperature variation being out of phase (OP), and the minimum strain reached quickly. Prolonged higher temperatures lead the strain-temperature variation to be in-phase (IP). However, the cooling process reverses the order. The leading and trailing edges at the top section of the blade experience prolonged higher temperatures, leading to oxidative and creep damage [8].

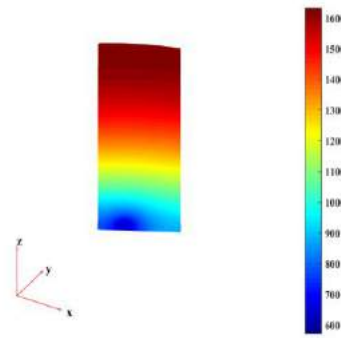


Figure 8: Finite element analysis of the steady state temperature distribution in the GT blade

The simulation results in Figure 9 show that the blade gains heat by conduction from the hot gases, increasing steadily. If the blades are not adequately cooled, the temperature of the blade could increase until the blade material melting point reaches, leading to blade damage from excessive temperatures. Figure 10 shows the convective cooling process as cool air passes through the blade. The cool air extracts heat from the blade through forced convection, and the temperature in the blade decreases rapidly to about 600°C. It brings the temperature within the safe operating limit of the blade. It emphasizes the need for effective cooling methods during turbine blade operation, which conforms to the findings of [20].

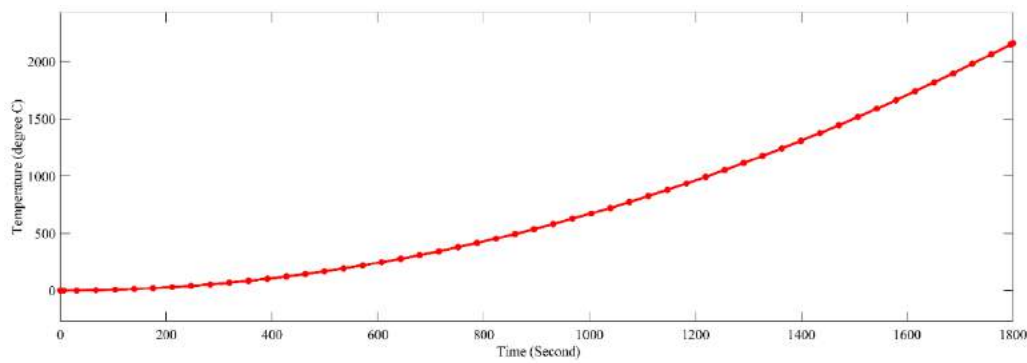


Figure 9: Temperature profile of heat transfer by conduction in the GT blade at 1800s duration

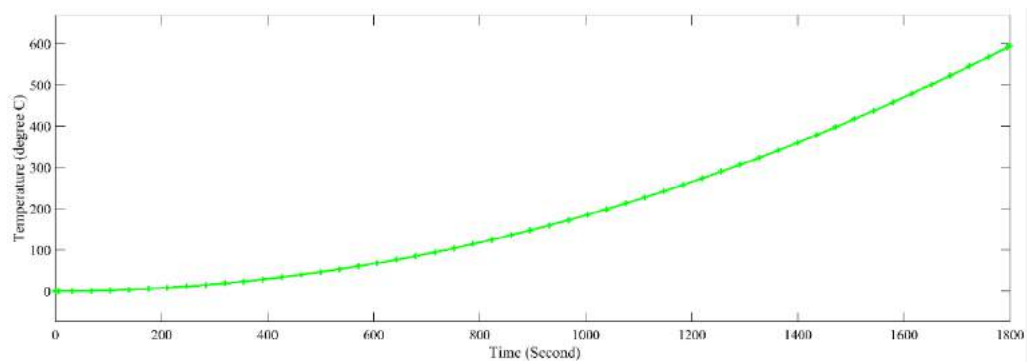


Figure 10: Temperature profile for the convective heat transfer in the GT blade at 1800s duration

The heat transfer models of the cold and hot sides were simulated using Simulink, as shown in Figure A1 (a) and (b), and the graphs showing the relationship between the heat transfer coefficient (HTC), Reynold's number (Re), and the absolute velocities, obtained for the hot and cold sections of the blade are in Figure 11 and Figure 12. At higher velocities, the viscosity of the cold air is low, and the heat transfer coefficient would be high. Hence, Figure 11 shows a steady increase in both Reynold's number and heat transfer coefficient as the velocity increases at the cold section of the blade. Heat transfer coefficient is a significant factor in convective heat transfer [17]. Figure 12 illustrates the graph of the HTC, Reynold's number, and absolute velocity for the hot section. It showed that an increase in velocity results in a consequent increase in Reynold's number; however, there is a steady decrease in the heat transfer coefficient, which could result from the high-temperature difference at the hot section of the blade. The turbulent intensities at the hot section of the blade may also have caused the decrease in the heat transfer coefficient [21].

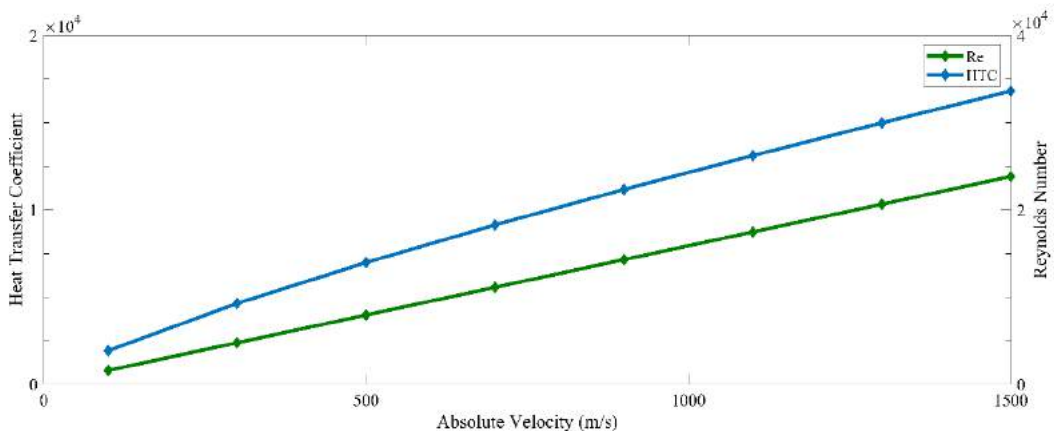


Figure 11: The effect of absolute velocity on Heat Transfer Coefficient and Reynolds Number (Cold Side)

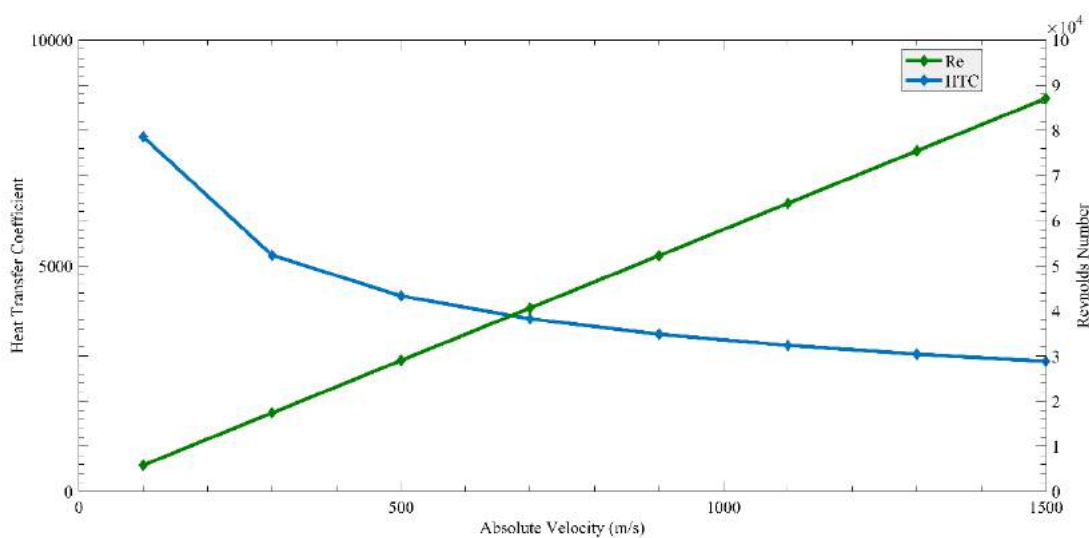


Figure 12: The effect of absolute velocity on Heat Transfer Coefficient and Reynolds Number (Hot Side)

The finite element analysis showing the stress distribution across the blade span is in Figure 13. It shows that higher stresses are experienced from the root to the blade's tip, with lower stresses acting from the leading edge to the trailing edge at the top of the blade. The stress-speed relationship is in Figure 15. As the turbine speed increases, the centrifugal tensile stress also increases. High cyclic stresses in the turbine blade could suggest the formation of microcracks within the material grain boundaries which could lead to creep damage [8].

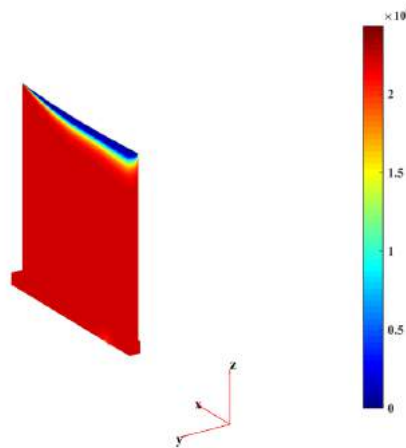


Figure 13: Finite element analysis of the steady state stress distribution in the GT blade

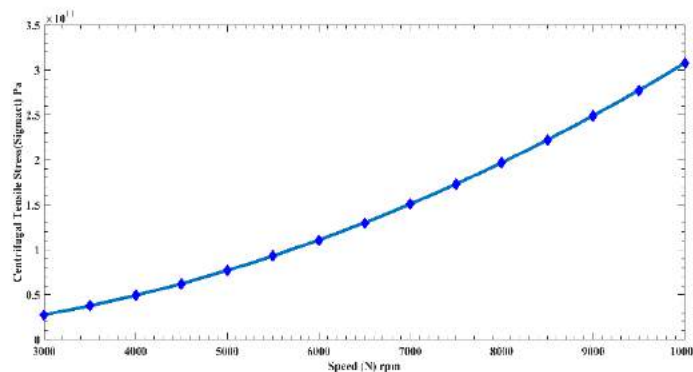


Figure 14: Stress-Speed relationship of a HP gas turbine blade

4. Conclusion

The study successfully modelled the TMF behavior of a turbine blade made of IN738LC using FEM and examined the blade's thermal and stress distributions and heat transfer. The finite element predicted the temperature and stress distributions in the blade, illustrating the sections of the blade that are susceptible to damage during thermomechanical fatigue. Fourier's law of heat conduction and Newton's law of cooling equations predicted the heat transfer process of the interaction between the hot gases and cooling air in the blade. It also modelled the heat transfer coefficient for the blade's hot and cold sections and obtained the heat transfer coefficients, Reynold's number, and Stanton

number at different velocities on the hot and cold section of the blade. The study established the Heat transfer coefficient and Reynold's number relationship with the change in velocities at the hot and cold sections of the blade. The stress model computed the centrifugal tensile stress arising from the high rotational speed, which would be used for TMF calculations to predict the creep life of the blade. Therefore, the finite element method is suitable for studying the thermomechanical fatigue of turbine blade metals, a prerequisite to blade life predictions.

Nomenclature

A	Heat transfer surface area (m ²)
A _b	Annulus area (m ²)
A _g	Hot gas cross sectional area (m ²)
C	Specific heat capacity of the blade material (J/kg.°C)
C _b	Chord of the blade (m)
c _{pg}	Specific heat at constant pressure (J/kg.°C)
D _h	Hole diameter (m)
D _m	Mean blade row diameter (m)
H	Blade height (m)
h _{cs}	Heat transfer coefficient at the cold side of the blade (W/m ² K)
h _g	Heat transfer coefficient (W/m ² K)
k	Coefficient of thermal diffusivity (m ² /s)
K _{cs}	Thermal conductivity of the cold air (W/m.K)
m _g	Gas mass flow (kg)
N	Rotational speed (rpm)
NU _{cs}	Nusselt number
Pr _g	Prandtl number
q	Heat flux (W/m ²)
q'	Heat transfer rate (kJ/kW.hr)
Re _{cs}	Reynold's number of the cold air
Re _g	Reynold's number of the hot gas
St _g	Stanton number
T	Temperature in the blade (°C)
T _g	Temperature of the hot gas (°C)
T _w	Wall metal temperature (°C)
V _{abscs}	Absolute velocity of the cold air (m/s)
V _{absg}	Absolute velocity of the hot gas (m/s)

Greek letters

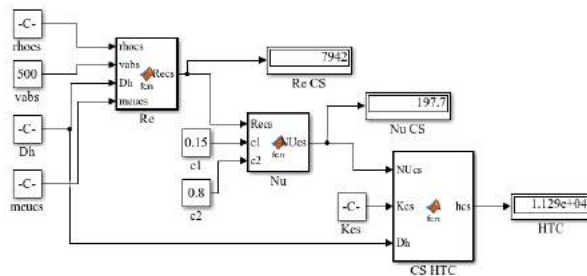
α ₂	Flow outlet angle (deg)
μ _{cs}	Kinematic viscosity of the cold air (m ² /s)
μ _g	Kinematic viscosity of the hot gas (m ² /s)
ρ	Density of the blade material (kg/m ³)
ρ _b	Density of the blade material (kg/m ³)
ρ _{cs}	Density of air on the cold side of the blade (kg/m ³)
ρ _g	Density of hot gas (kg/m ³)
(σ _{ct}) _{max}	Maximum centrifugal tensile stress (MPa)

References

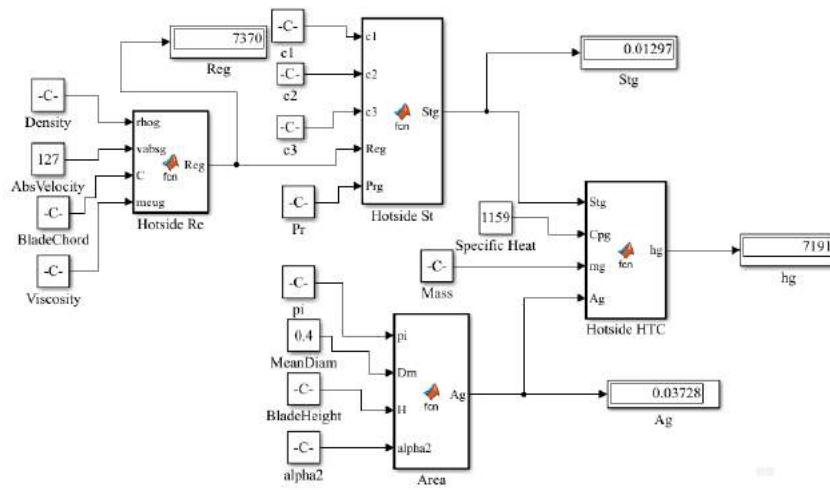
- [1] P. P. Walsh & P. Fletcher (2004). *Gas Turbine Performance*, 2nd Ed. United Kingdom: Blackwell Science Ltd.
- [2] M. P. Boyce (2012). *Gas Turbine Engineering Handbook*, 4th Ed. USA: Elsevier Inc.
- [3] G. Tony (2009). *Gas Turbine Handbook: Principles and Practice*, 4th Ed. USA: The Fairmont Press, Inc.
- [4] W. Sanz (2008). "Design of Thermal Turbomachinery," pp. 1–41.
- [5] K. A. B. Pathirathna (2013). "Gas Turbine Thermodynamic And Performance Analysis Methods Using Available Catalog Data," University of Gavle.

- [6] K. Kanagaraja, G. Jegadeeswari, and B. Kirubadurai (2019). "Optimization of Gas Turbine Blade Cooling System," *Int. J. Innov. Technol. Explor. Eng.*, vol. 8, no. 11, pp. 4176–4181.
- [7] A. Mazur Z., Luna-Ramirez A. J. A. and C.-A (2005). "Failure analysis of a gas turbine blade made of Inconel 738LC alloy," *Eng. Fail. Anal.*, vol. 12, no. 2005, pp. 474–486.
- [8] D. Socie and B. Socie (2007). "Thermomechanical fatigue made easy," in *6th Engineering Society International Conference on Durability and Fatigue*, pp. 1–15.
- [9] P. B. Stephen (2009) *Thermo-mechanical fatigue behaviour of the near-*. Berlin: BAM Bundesanstalt für Materialforschung und -prüfung Layout.
- [10] K. Y. Lee D, Lee J, Kim Y, Koo J, Seok C (2017). "Thermo Mechanical Fatigue Life Prediction of Ni-Based," *Int. J. Precis. Eng. Manuf.*, vol. 18, no. 4, pp. 561–566.
- [11] S. Rani (2018). "Common Failures in Gas Turbine Blade: A Critical Review," *Int. J. Eng. Sci. Res. Technol.*, vol. 7, no. 3, pp. 799–803.
- [12] H. V. E. Scheibel J. R., Aluru R (2017). "Mechanical Properties in GTD-111 Alloy in Heavy Frame Gas Turbines," *EPRI*, pp. 1–13.
- [13] S. G. and L. Y. Hyun J (2006). "Life Prediction of Thermo-Mechanical Fatigue for Nickel Based," *Key Eng. Mater.*, vol. 328, no. 2006, pp. 953–956.
- [14] D. Lee, I. Shin, Y. Kim, J. Koo, and C. Seok (2014). "Prediction of Thermo-Mechanical Fatigue Life of IN738 LC Using the Finite Element Analysis," *Int. J. Precis. Eng. Manuf.*, vol. 15, no. 8, pp. 1733–1737.
- [15] E. Fleury, & J. S. Ha (2001). "Thermomechanical fatigue behaviour of nickel base superalloy IN738LC Part 2 – Lifetime prediction," *Mater. Sci. Technol.*, vol. 17, no. August, pp. 1–8.
- [16] S. C. Chapra and R. P. Canale (2015). *Numerical methods for engineers*, 7th Ed. New York: McGraw-Hill Science/Engineering/Math.
- [17] L. M. Jiji (2006). *Heat convection*. Netherlands: Springer.
- [18] S. Eshati, P. Laskaridis, A. Haslam, and P. Pilidis (2012). "The Influence Of Humidity On The Creep Life Of A High Pressure Gas Turbine Blade : Part I Heat Transfer Model," in *Proceedings of ASME Turbo Expo 2012 GT2012*, GT2012-69455, pp. 1–11.
- [19] H. I. H. Saravanamuttoo, G. F. C. Rogers, H. Cohen, & P. V. Straznicky (2009). *Gas Turbine Theory*, 6th Ed. England: Pearson Education Limited.
- [20] K. Vaferi, M. Vajdi, S. Nekahi, and S. Nekahi (2020). "Thermo-mechanical simulation of ultrahigh temperature ceramic composites as alternative materials for gas turbine stator blades," *Ceram. Int.*, no. July, pp. 1–14.
- [21] H. Zirakzadeh (2014). "Numerical Investigation Of Temperature Distribution On A High Pressure Gas Turbine Blade," Texas A& M University.

Appendix



(a)



(b)

Figure A1 (a) Simulink Model For the Cold Side Heat Transfer; (b) Simulink Model for the Hot side Heat Transfer